Terra Nova

doi: 10.1111/ter.12074

F, Cl and S input via serpentinite in subduction zones: implications for the nature of the fluid released at depth

Baptiste Debret,[1,2,3] Kenneth T. Koga,[1,2,3] Christian Nicollet,[1,2,3] Muriel Andreani[4] and Stéphane Schwartz[5]

[1]*Clermont Université, Université Blaise Pascal, Laboratoire Magmas et Volcans, Clermont-Ferrand 63038, France;* [2]*CNRS, UMR6524, LMV, Clermont-Ferrand 63038, France;* [3]*IRD, R163, LMV, Clermont-Ferrand 63038, France;* [4]*Laboratoire de Géologie de Lyon, ENS - Université Lyon 1, Villeurbanne France;* [5]*Institut des Sciences de la Terre, Université Grenoble I, Grenoble France*

ABSTRACT

The abundances of F, Cl and S in arc magmas are systematically higher than in other mantle-derived magmas, suggesting that these elements are added from the slab along with H_2O. We present ion probe microanalyses of F, Cl and S in serpentine minerals that represent the *P–T* evolution of the oceanic lithosphere, from its serpentinization at the ridge, to its dehydration at around 100 km depth during subduction. F, Cl and S are incorporated early into serpentine during its formation at mid-ocean ridges, and serpentinized lithosphere then carries these elements to subduction zones. More than 50% of the F, Cl and S are removed from serpentine during the prograde metamorphic lizardite/antigorite transition. Due to the low solubility of F in water, and to the low amount of water released during this phase transition, the fluids mobilizing these elements must be dominated by SO_X rather than H_2O.

Terra Nova, 26, 96–101, 2014

Introduction

Serpentinites are a common constituent (up to 60%) of oceanic lithosphere (Cannat *et al.*, 2010). Because they contain up to 13 wt% water, and are thought to be stable down to a depth of 150 km in a typical subduction zone (e.g. Wunder and Schreyer, 1997), serpentinite dehydration at depth may modify the composition of the overlying mantle wedge, as well as the composition of the arc magmas derived from the wedge.

Primitive melt inclusions of arc magmas are enriched in F, Cl and S relative to MORB magmas (Métrich *et al.*, 1999; Straub and Layne, 2003). This suggests that these elements are released during slab dehydration or melting, and can potentially act as tracers of fluid phases in arc magma sources. Accurate assessments of the F, Cl and S budgets in subducting slabs are needed to determine the amounts of elements transferred from the slab to the sub-arc mantle and to the deep mantle.

At slow and ultra-slow spreading ridges, the mantle peridotites in the upper 3–6 km of the lithosphere are highly serpentinized to lizardite and chrysotile as a result of seawater circulation (Cannat *et al.*, 2010). This process causes an enrichment in trace elements (Kodolanyi *et al.*, 2012), Cl, S (Alt and Shanks, 2003) and F (Orberger *et al.*, 1999) in the serpentinites relative to unaltered peridotite. During subduction, the serpentinized oceanic lithosphere releases fluids via the transformation of chrysotile and lizardite to antigorite (at ~300 °C), and subsequently, at higher temperature (>500 °C), via the breakdown of antigorite to secondary olivine (Evans, 2004). Information on the nature and chemical composition of the fluid released during these two reactions is essential for a better understanding of arc magma composition and production at depth.

Previous studies have shown that Cl is transferred by fluids from the slab to arc magmas during serpentine phase changes (Kendrick *et al.*, 2011). Alt *et al.* (2012) suggested that the last stage of antigorite breakdown is also accompanied by S release, based on bulk-rock analyses. The behaviour of F, however, is poorly constrained in subduction zones: while arc magma studies suggest that F, Cl and S are transferred from the subducting slab (e.g. Le Voyer *et al.*, 2010), bulk-rock serpentinite data do not show any evidence for F loss during serpentine phase transitions (John *et al.*, 2011).

The aim of this study is to highlight the role of serpentinites in recycling F, Cl and S in subduction zones and to increase our understanding of the nature and composition of the released fluids. We report *in situ* measurements of halogen (F, Cl) and volatile element (S) concentrations in serpentines collected in a present-day oceanic setting and in the Western Alps ophiolites. These ophiolites represent highly hydrated and serpentinized fragments of the Jurassic Ligurian Ocean, recording metamorphic grades from greenschist to eclogite facies (Lagabrielle and Cannat, 1990).

Geological settings and petrographic study

Alpine ophiolites, resulting from the exhumation of fragments of Tethyan oceanic lithosphere during subduction and collision, are an analogue of the Atlantic Ocean lithosphere (Lagabrielle and Cannat, 1990) in which serpentinites are a major component (Cannat *et al.*, 2010). We sampled a serpentinite suite from Alpine ophiolites, which records different metamorphic conditions representing a subduction geothermal gradient from 10 to ~100 km depth (Fig. 1A, B). We compare them with a 'reference' oceanic serpentinite from the Mid-Atlantic Ridge (ODP sample). The different varieties of

Correspondence: Mr. Baptiste Debret, Laboratoire Magmas et Volcans, 5 rue Kessler, Clermont-Ferrand 63038, France. Tel.: 00 33 673 91 1019; e-mail: b.debret@opgc.univ-bpclermont.fr

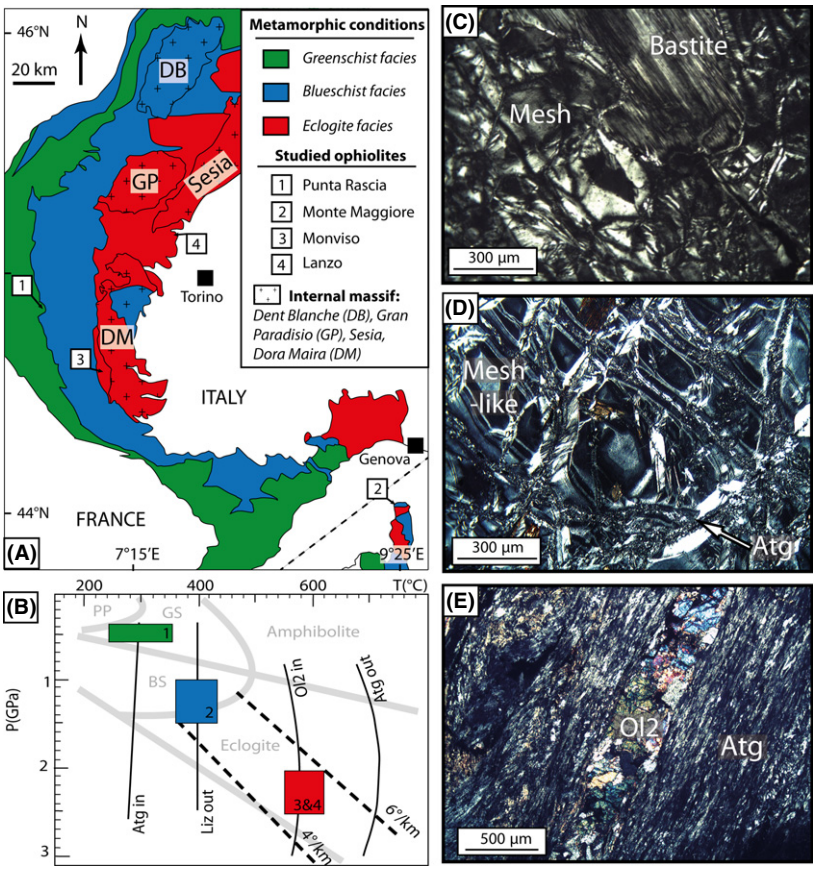

Fig. 1 (A) Simplified metamorphic map of the Western Alps showing the spatial distribution of the studied ultramafic ophiolites (numbered white squares). (B) *P–T* estimates of metagabbros from the studied ophiolites. The phase transitions are drawn from thermodynamical data (Evans, 2004; and references therein) and field observations (Schwartz *et al.*, 2013). Black dashed lines: subduction geotherms of 4 and 6 °C km^{-1}. Grey lines: metamorphic facies limits; PP: Prehnite-Pumpellyite, GS: Greenschist, BS: Blueschist. (C–E) Microphotographs of serpentinites from different metamorphic grades under crossed polarized light, illustrating the prograde evolution of serpentines. (C) Oceanic serpentinite (ODP sample) showing typical oceanic mesh and bastite texture. The mesh core consists of a grey homogeneous area delimited by fibrous rims. Bastite texture is composed of serpentine grains elongated parallel to the original mineral cleavages. (D) Monte Maggiore serpentinite showing a partially recrystallized mesh texture. The mesh-like rim is replaced by thin lamellae of antigorite (Atg). (E) Monviso serpentinite showing secondary olivine (Ol2) growth.

serpentine were identified in thin section, and characterized by Raman spectroscopy (Appendix S1).

The ODP sample is a fully serpentinized peridotite from the MARK area (leg 153-hole 920B). In this sample, lizardite is the dominant serpentine variety and is locally associated with chrysotile; it displays typical oceanic mesh or bastite textures replacing olivine or orthopyroxene (Fig. 1C).

The Punta Rascia ophiolite is located in the north of the Montgenèvre ophiolite. It is composed of metagabbro pods and serpentinites recording greenschist facies conditions (Fig. 1B; Mével *et al.*, 1978). At these *P–T* conditions, the transition of lizardite to antigorite is initiated locally by the partial recrystallization of oceanic mesh and bastite textures and by the growth of antigorite veins. The incomplete transition is inferred from mixed Raman spectra of lizardite and antigorite, defining 'mesh-like' and 'bastite-like' textures.

The Monte Maggiore ophiolite of Corsica is composed of serpentinized peridotites and metagabbros recording blueschist facies conditions (Fig. 1B; Vitale-Brovarone *et al.*, 2013). To the south of the massif, the peridotites are fully serpentinized into mesh- and bastite-like textures. The cores of the mesh- and bastite-like textures are each surrounded by a corona of thin antigorite lamellae (Fig. 1D) and are crosscut by antigorite veins.

The Monviso ophiolite is composed of foliated serpentinites and metagabbroic pods metamorphosed under eclogite facies conditions (Fig. 1B; Schwartz *et al.*, 2001). At these *P–T* conditions, the oceanic textures in the serpentinites are fully recrystallized into antigorite lamellae. Locally, the serpentinites are crosscut by C-S structures displaying secondary olivine in the C plane formed at peak metamorphic conditions by prograde antigorite breakdown (Schwartz *et al.*, 2013).

The Lanzo ophiolite is an eclogitized oceanic serpentinization palaeofront (Debret *et al.*, 2013a). It is composed of slightly serpentinized peridotites (SSP), preserving rare relicts of early lizardite veins, interpreted as being the first stages of oceanic peridotite serpentinization (Debret *et al.*, 2013a), and of foliated serpentinites fully recrystallized into antigorite during subduction. Locally, the serpentinites contain secondary olivines formed by antigorite breakdown at peak metamorphic conditions (Pelletier and Müntener, 2006, Fig. 1B).

Results

Fluorine, chlorine and sulphur compositions were measured using the CAMECA IMS 1270 ion probe at the CRPG (Nancy, France). Details of the methodology are given in Appendix S2; standard material and results are available in Appendices S3 and S4.

To constrain the behaviour of halogens and volatile elements during oceanic serpentinization, two samples representing different degrees of serpentinization were analysed: an SSP (degree of serpentinization <20%) from the Lanzo massif and a

serpentinite (degree of serpentinization ~100%) from the ODP borehole. Primary minerals in the SSP have low concentrations of F (1–21 p.p.m.), Cl (2–33 p.p.m.) and S (1–25 p.p.m.), while the oceanic serpentinization of the peridotite is marked by a progressive increase in these element concentrations in the serpentine. The lizardite veins in the SSP have higher concentrations of F (6–64 p.p.m.), Cl (490–10 578 p.p.m.) and S (32–216 p.p.m.) than the primary minerals, while the mesh and bastite textures (Fig. 1C) in the fully serpentinized peridotites (i.e. ODP samples) are enriched in F (50–319 p.p.m.) and S (270–989 p.p.m.), but display similar Cl (205–1056 p.p.m.) concentrations to those measured in SSP lizardite veins (Fig. 2).

The evolution of F, Cl and S contents in serpentine during subduction is represented by Alpine ophiolite samples of various metamorphic grades. In the serpentinites of greenschist and blueschist facies, mixed lizardite and antigorite assemblages have lower F (26–64 p.p.m.), Cl (54–1266 p.p.m.) and S (15–444 p.p.m.) concentrations than pure lizardite assemblages. In the same rocks, the late formation of pure antigorite veins is accompanied by a further decrease in F (23–40 p.p.m.), Cl (90–561 p.p.m.) and S (43–190 p.p.m.) concentrations relative to lizardite and lizardite-antigorite assemblages (Fig. 3). At eclogite facies, the pure antigorites have lower F (4–22 p.p.m.), Cl (20–428 p.p.m.) and S (9–103 p.p.m.) concentrations than the serpentines of lower metamorphic degrees. Secondary olivines (F = 1–2 p.p.m., Cl = 7–16 p.p.m., S = 1–8 p.p.m.) have a similarly low content to primary olivines (Fig. 3).

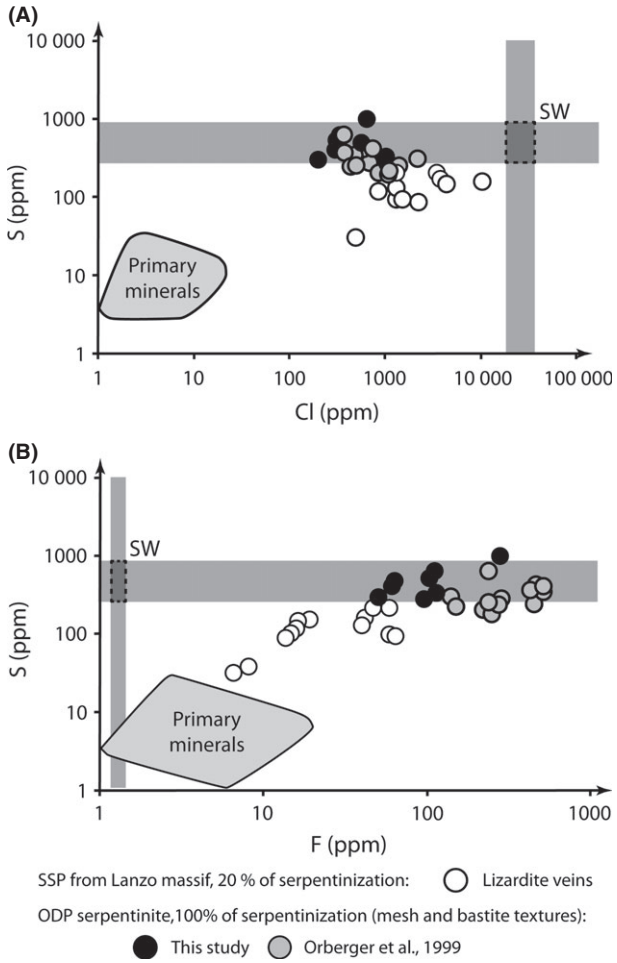

Fig. 2 Plots of element concentrations in serpentines (this study and Orberger *et al.*, 1999) of different textures and increasing degrees of hydration in relation to concentrations of primary minerals and hypothetical seawater concentration (A) S vs. Cl, (B) S vs. F). Ranges of element concentrations in primary minerals (olivine, orthopyroxene and clinopyroxene) from 1–21 p.p.m., 2–33 p.p.m. and 2–25 p.p.m. for F, Cl and S respectively; ranges of seawater (SW, grey bands) concentration are after Li (1991) and Douville *et al.* (1999); preferred values: F ~ 1.3 p.p.m.; Cl = 1.9–3.5 wt%, S = 300–900 p.p.m.. The crossing point of the concentration bands for seawater is assumed to represent the composition of the serpentinizing fluid. Symbol size corresponds to analytical uncertainty.

Discussion

The serpentinization process results from seawater circulation through the mantle exhumed at the ridge. It is accompanied by an increase in F, Cl and S concentrations in lizardite relative to the primary peridotite minerals (Fig. 2). Dissolution of pre-existing accessory phases in the peridotite (e.g. sulphides) cannot result in the observed positive correlation between F and S during the serpentinization process (Fig. 2B) because these phases are not F-bearing. Thus, the F, Cl and S increase in serpentine must be caused by seawater circulation during the serpentinization process.

Fluorine, chlorine and sulphur display different behaviours during oceanic serpentinization. The F content of serpentine is higher than that of seawater (Li, 1991) and increases with increasing degree of serpentinization (Fig. 2B). Thus, F is progressively scavenged by lizardite during fluid circulation and $D_F^{SW/serpentine}<1$ ($D_i = [X]_i^{SW}/[X]_i^{Serpentine}$; i: considered element, SW: sea water). During the initial stage of serpentinization, the F and S concentrations show a positive correlation; then, at higher degrees of serpentinization, the S concentration in serpentine does not increase beyond that of seawater (Fig. 2B). This suggests that the S concentration of serpentine results from interaction between primary minerals and seawater. Therefore, S addition during serpentinization is controlled by both

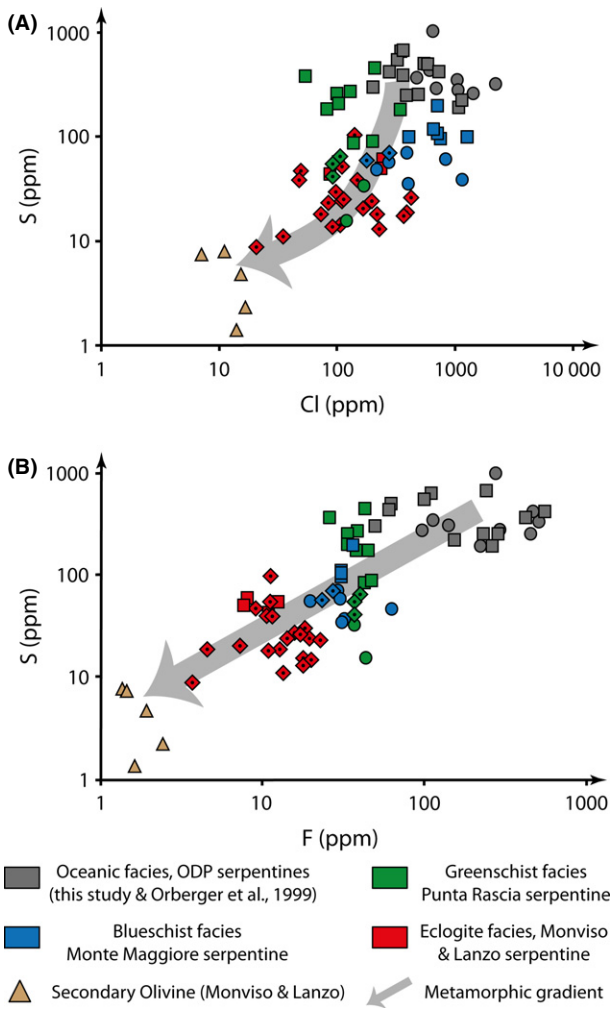

Fig. 3 Plots of element concentrations in serpentine polymorphs and secondary olivine, showing the evolution during prograde metamorphism due to subduction from their formation near the spreading ridge to their dehydration at eclogite facies conditions. (A) S vs. Cl. (B) S vs. F. The grey arrow indicates the compositional evolution associated with prograde metamorphism. Squares: mesh- and mesh-like textures; Circles: bastite- and bastite-like textures; Diamonds with centre point: antigorite. Samples are grouped according to their increasing metamorphic grade using the same colours as in Fig. 1.

seawater composition and the water/rock (W/R) ratio. The Cl concentration of lizardite is highly variable, but always lower than that of seawater (Fig. 2A). This suggests that, during the serpentinization process, Cl is rapidly incorporated into serpentine, and that saturation (or exchange equilibrium) is reached in the mineral before serpentinization reaches 20%, regardless of the position of Cl in the serpentine structure (as a hydroxyl group substitution or occurring in a weakly bound position).

The S and Cl addition during serpentinization is controlled by seawater composition, serpentine structure and other thermodynamic parameters such as fO_2 and T (Alt and Shanks, 2003; Bonifacie *et al.*, 2008; Delacour *et al.*, 2008). On the other hand, F addition is controlled by the local degree of serpentinization and, thus, mostly by the W/R ratio. Mass balance calculations based on F concentrations in serpentine, considering $D_F^{SW/serpentine} \ll 1$ and for a lherzolitic composition (20% pyroxene, 80% olivine), show an increase in W/R ratio from ~3 in the SSP to ~70 in the fully hydrated serpentinites. As the real F abundance in the serpentinizing fluids is unknown, seawater F concentration is used instead. Therefore, these W/R values should be considered as maximum estimates, because the serpentinizing fluid may contain more F than does seawater following potential interaction with MORB or sediments. However, it should be noted that this W/R ratio is in good agreement with a previous study where the W/R ratio has been shown to increase from ~0.6 to ~100 depending on local serpentinization degree (Andreani *et al.*, 2013).

During subduction, in passing from greenschist to eclogite facies, serpentinites change from lizardite-rich to antigorite-rich to antigorite with secondary olivine-bearing assemblages. This textural evolution is accompanied by a progressive decrease in the F, Cl and S contents of the remaining assemblages (Fig. 3). *In situ* analyses of fluid mobile elements in serpentines from the investigated ophiolites show that the serpentinites evolved from ridge to subduction without interaction with external fluids (Debret *et al.*, 2013b), as opposed to observations made in the accretionary prism (Lafay *et al.*, 2013; Fig. 1A). Furthermore, the selected samples correspond to peridotites that have largely been serpentinized during the oceanic stage (e.g. Debret *et al.*, 2013a). Therefore, the observed evolution in Fig. 3 does not reflect contamination or dilution processes during subduction. Instead, they suggest that, during prograde metamorphism, F, Cl and S are continuously released into a fluid phase that can metasomatize the overlying mantle wedge.

The results are in good agreement with arc magma studies (e.g. Le Voyer *et al.*, 2010) suggesting that F, Cl and S are transferred from the slab to the mantle wedge by fluids during prograde metamorphism. Different conclusions were obtained from bulk-rock analyses in John *et al.* (2011), where the analysed oceanic serpentinites have lower halogen concentrations than found in previous studies (~1000 p.p.m.; Barnes and Sharp, 2006; Bonifacie *et al.*, 2008). Our data, representing *in situ* halogen concentrations in serpentine during subduction, illustrate the chemical evolution during serpentine

phase changes more accurately than data from the whole rock evolution, which integrates several processes.

Of the two major phase transitions, the antigorite breakdown at around 150 km depth (Wunder and Schreyer, 1997) is the most significant source of H_2O. However, the decrease in halogen and volatile concentrations is more pronounced during the lizardite to antigorite transition than during antigorite breakdown (Fig. 3), showing that most of the fluid mobile (Vils *et al.*, 2011), volatile and halogen elements are removed in the first 70 km of subduction. This calls into question the nature of the fluid liberated during the first stage of subduction, because only a small amount of water is released during the lizardite to antigorite transition. Furthermore, this water release causes a new antigorite-bearing serpentinization of the slab (Debret *et al.*, 2013a), which reduces the amount of water actually transferred to the mantle wedge.

During oceanic serpentinization, from 300 to 400 °C, we expect that $D_F^{SW/serpentine} < 1$. This is in good agreement with experimental results where F partitioning between water and hydrous minerals ranges from 0.02 to 0.42 (Wu and Koga, 2013). In subduction zones, during the lizardite to antigorite transition, from 300 to 400 °C (Schwartz *et al.*, 2013), the progressive drop in F concentration proves that $D_F^{fluid/serpentine} > 1$. This implies a change in the nature of the fluid released during subduction. At the oceanic stage, S is mainly incorporated in micro-sulphides in serpentinites (Alt and Shanks, 2003). The observed drop in S during the lizardite to antigorite transition suggests that the released fluid is dominated by oxidized SO_X rather than by H_2O. This implies that the nature of the fluid released during the first stage of subduction might be controlled by redox reactions rather than dehydration reactions.

Out of the three elements studied, F is the only one controlled by the W/R ratio during oceanic serpentinization. Hence, it can be used for mass balance calculations in subduction zones. At slow spreading ridges, the serpentinite can comprise up to 60% of the upper 3.4 km of the oceanic lithosphere (Cannat *et al.*, 2010). Considering a subduction rate of 3 to 10 cm a^{-1}, the influx of F carried by serpentinites into subduction zones varies from 2.8×10^9 to 9.3×10^{10} kg (Ma km)$^{-1}$. On the other hand, considering an arc magma production rate of 35 to 95 km^3 (Ma km)$^{-1}$ (Dimalanta *et al.*, 2002) and a primary magma with a F content of ~600 p.p.m. (Lesser Antilles; Bouvier *et al.*, 2010), the outflux of F produced by magmatism in subduction zones ranges from 3.6×10^{10} to 1.1×10^{11} kg (Ma km)$^{-1}$. Thus, the serpentine reactions and breakdown during prograde metamorphism cannot, alone, explain the observed geochemical anomalies of arc magmatism. Other components in the oceanic lithosphere, such as sediments or meta-gabbros, must act as additional significant F reservoirs in subduction zones.

Acknowledgements

We thank E.R. Koga, E. Deloule, G. Van Den Bleeken and D. Magnin for their assistance during sample preparation and CAMECA IMS 1270 measurements. We acknowledge G. Fabbro for his correction of the English language, and G. Montagnac for Raman analyses. The Raman spectroscopy facility at the ENS Lyon is supported by CNRS INSU. This work was supported by ANR SlabFlux, ANR09BLAN033, CNRS-INSU funding attributed to LMV UMR 6524. This is Laboratory of excellence *ClerVolc* contribution n°72. We thank B. Evans and M. Marks for critical comments on an earlier version of this article, and for careful editorial handling by K. Mezger and M. Rahn.

References

Alt, J.C. and Shanks, W.C., III, 2003. Serpentinization of abyssal peridotites from the MARK area, Mid-Atlantic Ridge: sulfur geochemistry and reaction modeling. *Geochim. Cosmochim. Acta*, **67**, 641–653.

Alt, J.C., Garrido, C.J., Shanks, W.C., III, Turchyn, A., Padrón-Navarta, J.A., Sánchez-Vizcaíno, V.L., Gómez Pugnaire, M.T. and Marchesi, C., 2012. Recycling of water, carbon, and sulfur during subduction of serpentinites: a stable isotope study of Cerro del Almirez, Spain. *Earth Planet. Sci. Lett.*, **327-328**, 50–60.

Andreani, M., Muñoz, M., Marcaillou, C. and Delacour, A., 2013. μXANES study of iron redox state in serpentine during oceanic serpentinization. *Lithos*, **178**, 70–83.

Barnes, J.D. and Sharp, Z.D., 2006. A chlorine isotope study of DSDP/ODP serpentinized ultramafic rocks: insights into the serpentinization process. *Chem. Geol.*, **228**, 246–265.

Bonifacie, M., Busigny, V., Mével, C., Philippot, P., Agrinier, P., Jendrzejewski, N., Scambelluri, M. and Javoy, M., 2008. Chlorine isotopic composition in seafloor serpentinites and high-pressure metaperidotites. Insights into oceanic serpentinization and subduction processes. *Geochim. Cosmochim. Acta*, **72**, 126–139.

Bouvier, A.S., Deloule, E. and Métrich, N., 2010. Fluid inputs to magma sources of St. Vincent and Grenada (Lesser Antilles): new insights from trace elements in olivine-hosted melt inclusions. *J. Petrol.*, **51**, 1597–1615.

Cannat, M., Fontaine, F. and Escartin, J., 2010. Serpentinization and associated hydrogen and methane fluxes at slow spreading ridges. *Geophys. Monogr. Ser.*, **188**, 241–264.

Debret, B., Nicollet, C., Andreani, M., Schwartz, S. and Godard, M., 2013a. Three steps of serpentinization in an eclogitized oceanic serpentinization front (Lanzo Massif – Western Alps). *J. Metamorph. Geol.*, **31**, 165–186.

Debret, B., Andreani, M., Godard, M., Nicollet, C., Schwartz, S. and Lafay, R., 2013b. Trace element behaviour during serpentinization/deserpentinization of an eclogitized oceanic lithosphere: a LA-ICPMS study of the Lanzo ultramafic massif (Western Alps). *Chem. Geol.*, **357**, 117–133.

Delacour, A., Früh-Green, G.L. and Bernasconi, S.M., 2008. Sulfur mineralogy and geochemistry of serpentinites and gabbros of the Atlantis Massif (IODP Site U1309). *Geochim. Cosmochim. Acta*, **72**, 5111–5127.

Dimalanta, C., Taira, A., Yumul, G., Tokuyama, H. and Mochizuki, K., 2002. New rates of western Pacific island arc magmatism from seismic and gravity data. *Earth Planet. Sci. Lett.*, **202**, 105–115.

Douville, E., Bienvenu, P., Charlou, J.L., Donval, J.P., Fouquet, Y., Appriou, P. and Toshitaka, G., 1999. Yttrium and rare earth elements in fluids from various deep-sea hydrothermal systems. *Geochim. Cosmochim. Acta*, **63**, 627–643.

Evans, B.W., 2004. The serpentinite multisystem revisited: chrysotile is metastable. *Int. Geol. Rev.*, **46**, 479–506.

John, T., Scambelluri, M., Frische, M., Barnes, J.D. and Bach, W., 2011. Dehydration of subducting serpentinite: implications for halogen mobility in subduction zones and the deep halogen

cycle. *Earth Planet. Sci. Lett.*, **308**, 65–76.
Kendrick, M.A., Scambelluri, M., Honda, M. and Phillips, D., 2011. High abundances of noble gas and chlorine delivered to the mantle by serpentinite subduction. *Nat. Geosci.*, **4**, 807–812.
Kodolanyi, J., Pettke, T., Spandler, C., Kamber, B.S. and Gmeling, K., 2012. Geochemistry of ocean floor and fore-arc serpentinites: constraints on the ultramafic input to subduction zones. *J. Petrol.*, **53**, 235–270.
Lafay, R., Deschamps, F., Schwartz, S., Guillot, S., Godard, M., Debret, B. and Nicollet, C., 2013. High-pressure serpentinites, a trap-and-release system controlled by metamorphic conditions: example from the Piedmont zone of the western Alps. *Chem. Geol.*, **343**, 38–54.
Lagabrielle, Y. and Cannat, M., 1990. Alpine Jurassic ophiolites resemble to the modern central Atlantic basement. *Geology*, **18**, 319–322.
Le Voyer, M., Rose-Koga, E.F., Shimizu, N., Grove, T.L. and Schiano, P., 2010. Two contrasting H_2O-rich components in primary melt inclusions from Mount Shasta. *J. Petrol.*, **51**, 1571–1595.
Li, Y.-H., 1991. Distribution patterns of the elements in the ocean: a synthesis. *Geochim. Cosmochim. Acta*, **55**, 3223–3240.
Métrich, N., Schiano, P., Clocchiatti, R. and Maury, R., 1999. Transfer of sulfur in subduction settings: an example from Batan island (Luzon volcanic arc, Philippines). *Earth Planet. Sci. Lett.*, **167**, 1–14.
Mével, C., Caby, R. and Kienast, J.R., 1978. Amphibolite facies conditions in oceanic crust: example of amphibolitized flaser gabbros and amphibolites from the Chenaillet ophiolite massif (Hautes Alpes, France). *Earth Planet. Sci. Lett.*, **39**, 98–108.
Orberger, B., Métrich, N., Mosbah, M., Mével, C. and Fouquet, Y., 1999. Nuclear microprobe analysis of serpentine from the mid-Atlantic ridge. *Nucl. Instrum. Methods Phys. Res. B*, **158**, 575–581.
Pelletier, L. and Müntener, O., 2006. High-pressure metamorphism of the Lanzo peridotite and its oceanic cover, and some consequences for the Sezia-Lanzo zone (northwestern Italian Alps). *Lithos*, **90**, 111–130.
Schwartz, S., Allemand, P. and Guillot, S., 2001. Numerical model of the effect of serpentinites on the exhumation of eclogitic rocks: insights from the Monviso ophiolitic massif (Western Alps). *Tectonophysics*, **342**, 193–206.
Schwartz, S., Guillot, S., Reynard, B., Lafay, R., Debret, B., Nicollet, C., Lanari, P. and Auzende, A.L., 2013. Pressure–temperature estimates of the lizardite/antigorite transition in high pressure serpentinites. *Lithos*, **178**, 197–210.
Straub, S.M. and Layne, G.D., 2003. The systematics of chlorine, fluorine, and water in Izu arc front volcanic rocks: implications for volatile recycling in subduction zones. *Geochim. Cosmochim. Acta*, **67**, 4179–4203.
Vils, F., Müntener, O., Kalt, A. and Ludwig, T., 2011. Implications of the serpentine phase transition on the behaviour of beryllium and lithium-boron of subducted ultramafic rocks. *Geochim. Cosmochim. Acta*, **75**, 1249–1271.
Vitale-Brovarone, A., Beyssac, O., Malavieille, J., Molli, G., Beltrando, M. and Compagnoni, R., 2013. Stacking and metamorphism of continuous segments of subducted lithosphere in a high-pressure wedge: the example of Alpine Corsica (France). *Earth Sci. Rev.*, **116**, 35–56.
Wu, J. and Koga, K.T., 2013. Fluorine partitioning between hydrous minerals and aqueous fluid at 1 GPa and 770 – 947 °C: a New Constraint on Slab Flux. *Geochim. Cosmochim. Acta*, **119**, 77–92.
Wunder, B. and Schreyer, W., 1997. Antigorite: high-pressure stability in the system MgO-SiO_2-H_2O (MSH). *Lithos*, **41**, 213–227.

Received 30 March 2013; revised version accepted 9 September 2013

Supporting Information

Additional Supporting Information may be found in the online version of this article:

Appendix S1. Typical examples of Raman spectra of serpentine varieties. The grey band indicates the discriminating peaks of antigorite spectra compared with lizardite spectra. RAMAN spectroscopy was performed at the ENS Lyon. The Raman signal was acquired over approximately 90 s in three accumulating cycles, with a laser output power of 800 μW on the sample surface.

Appendix S2. Analytical method.

Appendix S3. Table of concentration calibration standards used in this study.

Appendix S4. SIMS analyses of minerals forming the slightly serpentinized peridotites and serpentinites

